Master Thesis (30 ECTS)

Predicting Human Running Kinematics from Joint Angles Measured with Stretch Sensors

Written by:

Lasse Kristoffer Taidal, 20165685
Niclas Hornbøll Rasmussen, 20163820
Øjvind Fredsgård Larsen, 20190723

Supervisor:
John Rasmussen, Professor, Aalborg University

4th semester, Sports Technology

Aalborg University

Department of Health Science and Technology

June 2021

Predicting Human Running Kinematics from Joint Angles Measured with Stretch Sensors

Lasse Kristoffer Taidal, Niclas Hornbøll Rasmussen & Øjvind Fredsgård Larsen

In collaboration with LEAP Technology ApS
4th semester Sports Technology, Aalborg University

We investigated LEAP Technology's stretch sensor's ability to measure joint angles in running in realistic conditions and the potential to generate a human running model from the data. From a database of 285 running trials, cross validation was utilized to identify relevant joint angles and their ability to provide input for Anybody Technology's running model. Using three stretch sensors, ankle and knee joint angles were measured and compared to Xsens MVN Link measurements. Stretch sensor kinematic data of one stride cycle were converted into Fourier series with 11 coefficients. Based on basic data (BD) and converted joint angles we sought to predict three running styles represented by 13 important kinematic variables. We found the relative prediction error (RPE) using BD and joint angle data from the knee stretch sensor to be 69.0% across 13 variables representing lower body extremities, posture and arms while RPE was 57.4% using BD and stretch sensor joint angle data from a posteriorly placed ankle sensor. Using only BD, RPE was 67.3%. In conclusion, based on 13 kinematic measures important for running, using a stretch sensor placed posteriorly on the ankle measuring the joint angle provided better predictions from the human running model when combining the data with BD than using only BD. However, the predictions are not sufficiently accurate.

0 INTRODUCTION

Public health is often mentioned in the context of physical activity with its health benefits including notable survival advantages and reduced risk of age-related disabilities [1]. Running is a way to incorporate physical activity into everyday routines and cardiovascular exercise is a factor in preventing lifestyle illnesses which cause a socioeconomic burden [2, 3]. However, in a meta-analysis, Andersson et al. [4], estimated that 79% of recreational runners experience annual running-related injuries (RRI) in the lower extremities [4]. The economical cost of RRI in the Netherlands was estimated by Hespanhol et al. [2] to the total cost of €173.72 per injury with the direct cost of health care treatment and the indirect cost of absenteeism from paid work [2]. Furthermore, it was found that runners tend to quit running after multiple RRI leading to absence of the health-related benefits [1, 5]. RRI etiology is well investigated but results are ambiguous with no single direct cause identified [2, 3, 4, 6, 7, 8, 9].

The biomechanical influence on RRI is not fully understood. It is established that an accumulated weekly running distance >65 km per week increases the risk of RRI significantly [4, 8], indicating a connection between cumulative load and injury frequency, while stride length and cadence has an ambiguous impact on RRI with no overall significant connection when not associated with other parameters [6, 9]. Investigations on the influence of foot strike pattern on RRI are inconclusive, since studies were carried out retrospectively [4, 5]. However, previous studies have not been able to exclude the biomechanics of running as a contributor to RRI. Andersson et al. [4] point out that a combination of the listed parameters contributes to RRI, and therefore a holistic perspective on running biomechanics is necessary. Therefore, it is still relevant to investigate the kinematics of running.

The current gold standard of estimating running kinematics is via optical motion-capture-systems in dedicated laboratory environments. However, it is expensive and inconvenient to collect data in laboratory environments and the accessibility for the general sports enthusiast is minimal [10, 11]. A parametric running model [12] was developed from running data collected with an optical motion-capture system. Data were then imported to The Anybody Modeling System (Anybody Technology A/S, Aalborg, Denmark) and converted to Fourier series consisting of 11 coefficients [12, 13]. The running model can via principal component analysis (PCA) and quadratic optimization predict a running style if some parameters are known in advance [12]. These parameters can be measured by different wearable devices to enhance the precision of the running model. This will make it possible for everyone to get an estimate of their biomechanics during running.

Mobile biofeedback has been made more accessible by incorporating wearable technology into everyday routines [14]. Wearables allow monitoring the impact of different terrain and running biomechanics [10]. Inertial measurement units (IMU) are used in sports wearables for performance monitoring, but also shows potential for injury monitoring. However, to measure joint angles with this technology, multiple IMU are required, unlike LEAP Technology's stretch sensor [15].

LEAP Technology ApS have developed a wearable stretch sensor which measures capacitance and has potential as a motion capture device [16]. The stretch sensor enables possibilities of measuring joint angles as input for generating the running model along with anthropometric measurements, running cadence, running speed and age. Tatora et al. [17] suggested using stretch sensors as wearables for monitoring joint angles. A worst-case root mean square error (RMSE) of 4° was found when monitoring knee and ankle movement [17].

The possibility to generate a running model and predict running style with parameters known in advance combined with the opportunity to incorporate a user-friendly wearable motion capture device is appealing. Therefore, the purpose of this study was to investigate LEAP Technology's stretch sensor's ability to measure joint angles in a real-world environment in relation to generating a human running model.

1 Method

1.1 Identifying relevant joints for measurement with stretch sensors

The statistical running model was based on data from 79 subjects (30 females, 49 males) and consisted of 285 running trials spread out on all subjects. The dataset contained anthropometric measures, information about running cadence and velocity for each trial and 1188 Fourier coefficients associated with 108 kinematic measures such as joint angles and accelerations of different parts of the body. To evaluate the precision of the predictions from the running model, cross validation was utilized. The validation set consisted of the trials from one subject at a time whereas the training set consisted of the remaining trials from the remaining subjects. To identify relevant joint angles as input for the running model when predicting running style, cross validation was done 11 times. Basic data (BD) consisting of running speed, angular stride frequency (ω), body height, body weight, body mass index (BMI), gender and age were given as input for every cross validation. Furthermore, six joint angles were given as input in different combinations. The joint angles were: Hip-, knee- and ankle flexion in the sagittal plane for both left and right leg cf. table 1.

Subsequently, the relative prediction error (RPE) for each kinematic parameter was calculated as follows:

$$
\begin{aligned}
PE_{i,l} &= \int_0^{\frac{2\pi}{\omega_i}} |FS_{orig,i,l} - FS_{pred,i,l}| \\
RPE(\%)_l &= \frac{\sum_{i=1}^{n} \frac{PE_{i,l}}{\int_0^{\frac{2\pi}{\omega}} |FS_{orig,i,l}|}}{n} \cdot 100\%
\end{aligned} \tag{1}
$$

where PE_i, l is the prediction error for trial i and kinematic parameter l, ω is the angular stride frequency for trial i, $FS_{orig,i,l}$ is the Fourier series representing the original kinematic data for trial i and kinematic parameter l, $FS_{pred,i,l}$ is the Fourier series representing the predicted kinematic data for trial i and kinematic parameter l and n is the number of trials.

The RPE for each kinematic parameter was further investigated across three categories; category 1: Lower extremities, category 2: Posture, category 3: Arms, cf. Appendix 1. This enabled transparency to which the input combinations of joint angles estimated different body regions. The cross validation formed the basis of choosing the joint angles to measure with stretch sensors.

Table 1: *Cross validation across three categories (Cat.) using different joint angles as input for the running model. Cat. 1 = Lower extremities, Cat. 2 = Posture, Cat. 3 = Arms, All = Full body, RPE = Relative prediction error (%), R = Right, BD = Basic data.*

RPE (%)	**Cat. 1**	**Cat. 2**	**Cat. 3**	**All**
Basic data	42.2	54.7	66.3	53.7
Hips+BD	38.8	54.8	72.3	53.6
Knees+BD	39.4	54.7	70.6	53.8
Ankles+BD	39.8	57.2	70.4	55.4
Hips Knees Ankles+BD	38.7	62.3	84.0	60.2
R Hip Knee Ankle+BD	37.1	57.1	72.7	54.9
R Hip Knee+BD	38.3	54.5	69.6	53.1
R Hip Ankle+BD	43.2	56.5	60.9	53.0
R Knee Ankle+BD	43.5	56.5	61.1	53.1
R Knee+BD	38.7	53.5	66.9	52.4
R Ankle+BD	39.1	54.7	66.4	53.0

1.2 Data collection

Running kinematic data of three healthy male subjects were collected. All were recreational runners. Subject information is presented in table 2. The number of participants was affected by the Covid-19 situation of the time of data collection, 2021 February-June.

Table 2: *Demographics for participating subjects.*

	Subject 1	**Subject 2**	**Subject 3**
Gender	Male	Male	Male
Age	26 years	25 years	25 years
Height	189 cm	179 cm	187 cm
Weight	90 kg	80 kg	75 kg

Prior to running trials, each subject was equipped with Xsens MVN Link Lycra suit (full body, 17 IMU) and three LEAP Technology stretch sensors connected to an electronic hardware device, which streamed the signal via bluetooth, cf. figure 1. For measuring ankle joint angles, two stretch sensors were used. Dimensions: length of 220 mm of which the stretchable zone was 100 mm, width of 20 mm and thickness of 0.4 mm. For measuring knee joint angles, a custom made stretch sensor was used. Dimensions: length of 320 mm, of which the stretchable zone was 200 mm, width of 20 mm and thickness of 0.4 mm. A stretch of 100% of the stretchable zone was allowed. The hip joint was excluded due to complications with sensor attachment and individual soft tissue artifacts.

Fig. 1: *Attachment of stretch sensors and a subject wearing Xsens MVN Link.*

The knee joint sensor (K) was placed on the anterior side of the right knee joint, one end on the tibial tuberosity and the other end on the thigh, to ensure that the sensor covered the entire knee joint. The other stretch sensors were placed on the right ankle joint, one anteriorly and one posteriorly. The anterior ankle joint sensor (AA) was placed with one end on the area above the navicular bone and the other end on the shin. The posterior ankle joint sensor (PA) was placed with one end on the inferior calcaneus and the other end on the calf. K was attached with the subject standing in an upright position with the knee fully extended. AA and PA were attached when the ankle was fully dorsiflexed and plantar flexed, respectively. When attached, all sensors were pre-stretched to ensure no slack.

Subsequently, the subject performed a short self-organized warm-up followed by a calibration procedure for both Xsens and the stretch sensors. To calibrate Xsens all recommended anthropometrics were measured and Npose+walking was used for calibration [18]. Calibration of the stretch sensors was performed using Xsens for measuring joint angles in different positions. Two calibration files were recorded for both the stretch sensors and Xsens, one for the knee and one for the ankle. For the knee, the subject was instructed to stand in a position with the knee fully extended and then change the knee angle 6-10 times separated by two second intervals. The procedure for the knee was repeated for the ankle starting with the ankle fully plantar flexed and the foot on the ground. Each subject then performed six trials divided into three running styles; 1) Low knee flexion (LF), 2) High knee flexion (HF) and 3) Forefoot running (FF), cf. figure 2. The trials were recorded during steady state on a flat, straight asphalt road in an urban environment. A running distance of 70 m was recorded. The subjects were free to choose their running speeds. Data were collected using MVN Analyze Pro 2021.0 and LEAP Technology Sensor Electronics Software. Kinematics were recorded with a sampling frequency of 240 Hz for Xsens and 250 Hz for the stretch sensors.

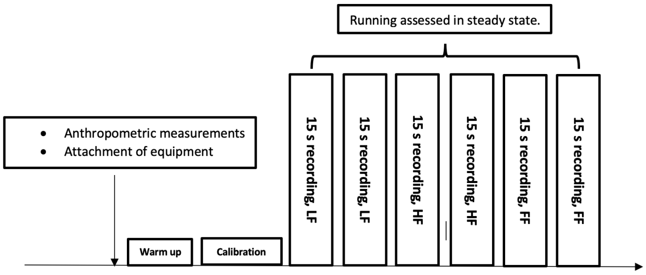

Fig. 2: *Test protocol. AA = Anterior ankle joint sensor, PA = Posterior ankle joint sensor, K = Knee joint sensor, LF = Low knee flexion, HF = High knee flexion, FF = Forefoot running.*

1.3 Data processing

1.3.1 Initial processing of running kinematics

Xsens data were HD-processed, which included filtering of the data, and joint angles were exported as .xlsx files through Xsens' software, MVN Analyze Pro 2021.0 [19]. Stretch sensor data were saved as .txt files. All data were imported to MatLab (2021a, The MathWorks Inc, Massachusetts, USA). In MatLab, stretch sensor data were filtered using a fourth order low-pass bi-directional butterworth filter with a cut-off frequency of 15 Hz [20]. Stretch sensor data were then resampled to 240 Hz in order to time normalize data.

To convert stretch sensor output from capacitance to joint angles the calibration files were utilized. For each of the joint angles measured during calibration, a mean of the central one second period, of the two second period where the position was held, was calculated for both the joint angles measured using Xsens and the capacitance measured using the stretch sensors. A second order polynomial was then fitted to the calibration dataset with joint angles as the dependent variable and capacitance as the independent variable. The quadratic function for the second order polynomial was then utilized to convert the stretch sensor data from capacitance to joint angles. This procedure was done for each sensor measurement on each subject resulting in nine different quadratic functions. Coefficients of determination (R^2), RMSEs and maximum absolute differences (MAD) between LEAP and Xsens were calculated for all three sensor measurements for the calibration files. Subsequently, shared start- and end points for both measurement methods were manually investigated for each trial and used as reference points for synchronization. From each trial a typical stride cycle was manually selected. The stride cycle represented the period from right heel strike to right heel strike. This period was identified using MVN Analyze Pro. RMSE was calculated for the typical stride cycle for all running styles. RMSE was used to determine which ankle sensor showed the most precise results. Only the ankle sensor with the most precise results was subject to further analysis.

The stretch sensor data for the period of the typical stride cycle was converted to Fourier series using the curve fitting application in MatLab. Each Fourier series consisted of 11 Fourier coefficients and ω was determined from the time of the stride cycle [13].

1.3.2 Prediction using running model

The Fourier coefficients were used as input in the running model [12]. The output from the running model was used as input in The AnyBody Modeling System to generate predicted full body kinematics. If the running model predicted unrealistic full body kinematics, fewer Fourier coefficients were given as input in the running model until realistic full body kinematics were present, based on visual feedback from The AnyBody Modeling System. To compute the actual full body kinematics, Xsens data were exported as Biovision Hierarchy (BVH) files and imported in The AnyBody Modeling System. 13 variables were chosen to evaluate the predicted running kinematics across the two measurement methods. Variables were flexion for ankle, hip, knee, elbow, and shoulder for both right and left side, relative rotation between pelvis and thorax, relative lateral bending between pelvis and thorax, and relative extension between pelvis and thorax. The 13 variables represented the three categories previously described, cf. section 1.1.

2 Results

2.1 Cross validation

Table 1 presents results from the cross validation. When excluding the hip joint, the running model made the best overall predictions of running style using right knee joint + BD with a RPE of 52.4%, whereas ankles + BD predicted with a RPE of 55.4%, being the worst prediction. RPE for category 1 was 38.7% for right knee + BD and 39.1% for right ankle + BD as the two best inputs. Using BD, RPE for category 1 was 42.2% and for all parameters 53.7%.

2.2 Calibration

The second order polynomial fit showed R^2-values ranging from 0.981 to 0.999. All R^2-values are listed in table 3. Figure 3 illustrates capacitance converted to joint angles compared to the Xsens measurements for subject 3. RMSE(MAD) for the three sensor placements across all subjects ranged from 0.68° (1.35°) to 2.99° (10.10°), cf. table 4.

Table 3: *R^2-values across calibrations files for all three subjects. K = Knee joint sensor, PA = Posterior ankle joint sensor, AA = Anterior ankle joint sensor.*

R^2-values	Subject 1	Subject 2	Subject 3
K	0.995	0.992	0.998
PA	0.999	0.992	0.996
AA	0.996	0.996	0.981

Table 4: *Root mean square error (RMSE) and maximum absolute difference (MAD) for all calibration files. K = Knee joint sensor, PA = Posterior ankle joint sensor, AA = Anterior ankle joint sensor.*

RMSE(MAD) (°)	Subject 1	Subject 2	Subject 3
K	2.38 (5.66)	2.99 (10.10)	1.15 (5.33)
PA	1.05 (3.95)	1.15 (4.17)	1.17 (3.33)
AA	1.09 (4.13)	0.68 (1.35)	2.67 (8.07)

2.3 Kinematic measures

Kinematic output for subject 3 collected with the stretch sensors and Xsens is illustrated in figure 4. Remaining subject kinematics are presented in Appendix 2. RMSE for all three sensors across running styles are listed in table 5. RMSE for K averaged 11.5°, for PA 7.3° and for AA 8.7°. For K RMSE ranged from 8.7° to 14.7° for LF and HF, respectively. RMSE ranged from 6.8° to 7.6° for PA for FF and LF/HF, respectively. RMSE ranged from 7.9° to 9.5° for AA for LF and HF, respectively. PA had lower RMSE for all types of running compared to AA.

2.4 Conversion to Fourier series

The transition of kinematic data from time series to Fourier series is illustrated in figure 5 and shows related R^2-values for PA and K in table 6. R^2-values for Fourier series conversion ranged from 0.980 to 0.996 for subject 1, from 0.979 to 0.999 for subject 2 and from 0.971 to 0.995 for subject 3.

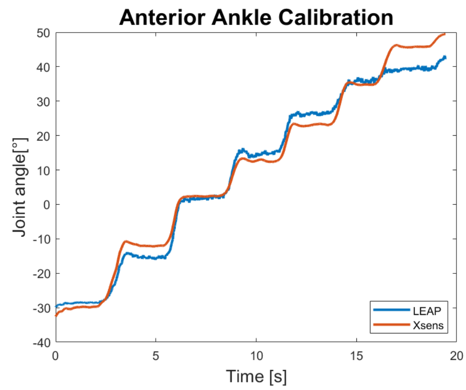

(a) *Calibration for AA, dorsiflexion. Subject 3.*

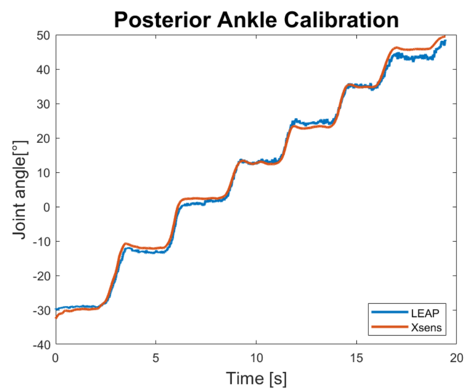

(b) *Calibration for PA, dorsiflexion. Subject 3.*

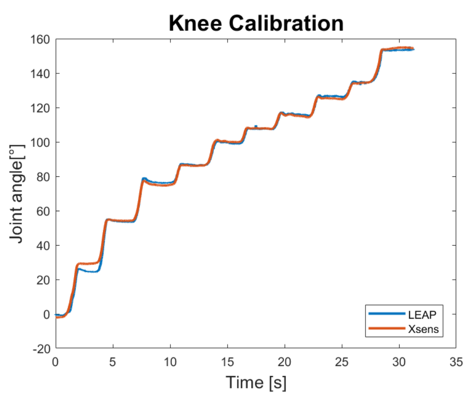

(c) *Calibration for K, flexion. Subject 3*

Fig. 3: *Calibration files. AA = Anterior ankle joint sensor, PA = Posterior ankle joint sensor, K = Knee joint sensor. Subject 3.*

2.5 Running model predictions

Table 7 presents RPEs for the 13 kinematic variables, listed in section 1.3.2, for all three running styles individually and combined. For combined running styles the mean RPE for all 13 variables was 57.4% for prediction using PA + BD, 69.0% for prediction using K + BD and 67.3% for prediction using only BD. For all running styles, predictions using PA showed lower RPE than predictions using K. Figure 6 illustrates the kinematics during one stride cycle for the actual running style, predictions using K + BD, predictions using PA + BD and predictions using only BD.

Table 5: *Root mean square error (RMSE) across running styles for all three sensors. K = Knee joint sensor, PA = Posterior ankle joint sensor, AA = Anterior ankle joint sensor*

RMSE (°)	LF	HF	FF	All
K	8.7	14.7	11.1	11.5
PA	7.6	7.6	6.8	7.3
AA	7.9	9.5	8.1	8.7

Table 6: *R^2-values across Fourier series conversions for all three subjects. K = Knee joint sensor, PA = Posterior ankle joint sensor, LF = Low knee flexion, HF = High knee flexion, FF = Forefoot running.*

R^2-values	Subject 1	Subject 2	Subject 3
K LF	0.994	0.999	0.993
PA LF	0.980	0.993	0.971
K HF	0.996	0.996	0.995
PA HF	0.985	0.986	0.976
K FF	0.995	0.998	0.995
PA FF	0.987	0.979	0.987

3 Discussion

The aim of this study was to investigate LEAP Technology's stretch sensor's ability to measure joint angles in a real-world environment in relation to generating a human running model. The findings of the current study were that RPE using K + BD was 69.0% across 13 variables representing lower body extremities, posture and arms while RPE was 57.4% using PA + BD. Using only BD, RPE was 67.3%, cf. table 7. This shows that using PA + BD reduced the RPE by 9.9 percentage points, while using K + BD increased the RPE by 1.7 percentage points. This indicates that the use of K + BD in the constellation of this study was not beneficial for generating the human running model, while PA + BD was beneficial, when looking only at the 13 variables selected in the current study.

3.1 The relevance of joint angle input in the running model

When studying table 1 it is clear that RPE for all combinations of input were above 50% which means that there was a large discrepancy between the predictions from the running model and the actual running style. Furthermore, it is interesting that a greater amount of input in the running model, e.g. hip-, knee- and ankle flexion for both sides combined with BD (RPE = 60.2%), did not provide better predictions in general. These findings emphasize the importance of the input provided to the running model. However, combining BD with certain joint angles did provide better predictions than using only BD. In this study, 10 different joint angle combinations were investigated of which six combinations provided better overall predictions. As

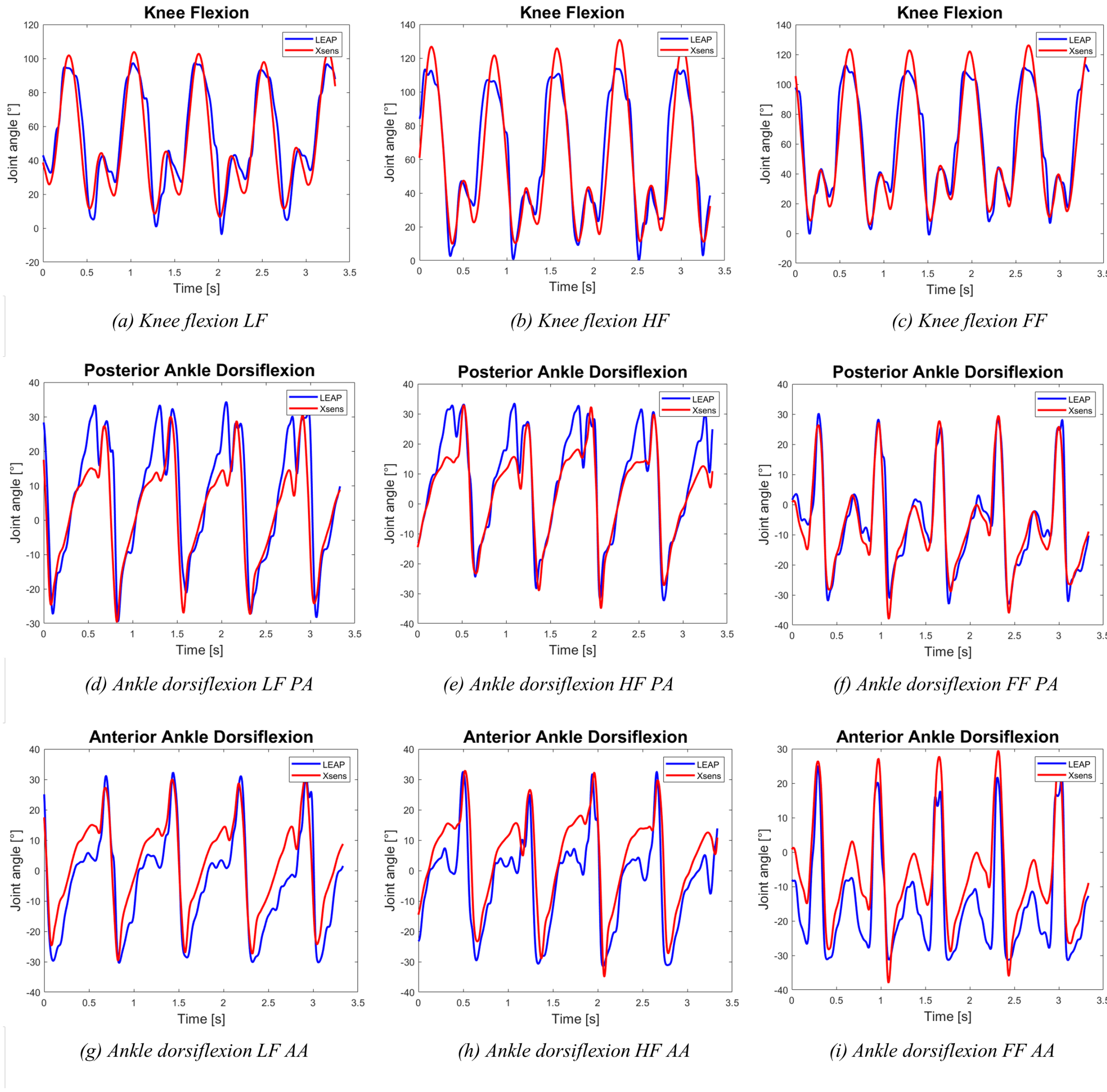

(a) *Knee flexion LF* (b) *Knee flexion HF* (c) *Knee flexion FF*

(d) *Ankle dorsiflexion LF PA* (e) *Ankle dorsiflexion HF PA* (f) *Ankle dorsiflexion FF PA*

(g) *Ankle dorsiflexion LF AA* (h) *Ankle dorsiflexion HF AA* (i) *Ankle dorsiflexion FF AA*

Fig. 4: *Joint angles histories from subject 3, for all three running styles from stretch sensors (LEAP) and Xsens over a period of 3.5 seconds. Remaining subject kinematics are presented in Appendix 2. LF = Low knee flexion, HF = High knee flexion, FF = Forefoot running, PA = Posterior ankle joint sensor, AA = Anterior ankle joint sensor.*

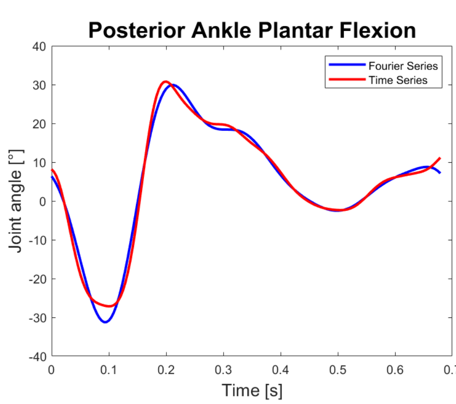

Fig. 5: *Kinematic data and the corresponding Fourier series with 11 coefficients for posterior ankle plantar flexion.*

mentioned in section 2.1, the right knee + BD provided the best overall predictions with a RPE of 52.4% being 1.3 percentage points better than using only BD (RPE = 53.7%). When focusing on category 1 the prediction was 3.5 percentage points better, cf. table 1.

These predictions were not particularly good. However, considering the number of subjects (79) and trials (285) in the running model it becomes clear that the running model was based on a limited amount of data. Increasing the number of subjects and the number of trials would most likely provide better predictions. Therefore, the RPE would decrease when increasing the amount of data and the relevance of providing joint angle histories in the running model would presumably increase. Furthermore, kinematic input from other wearables could in combination with joint angle histories provide better predictions. If the wearable could measure kinematics related to either posture of the

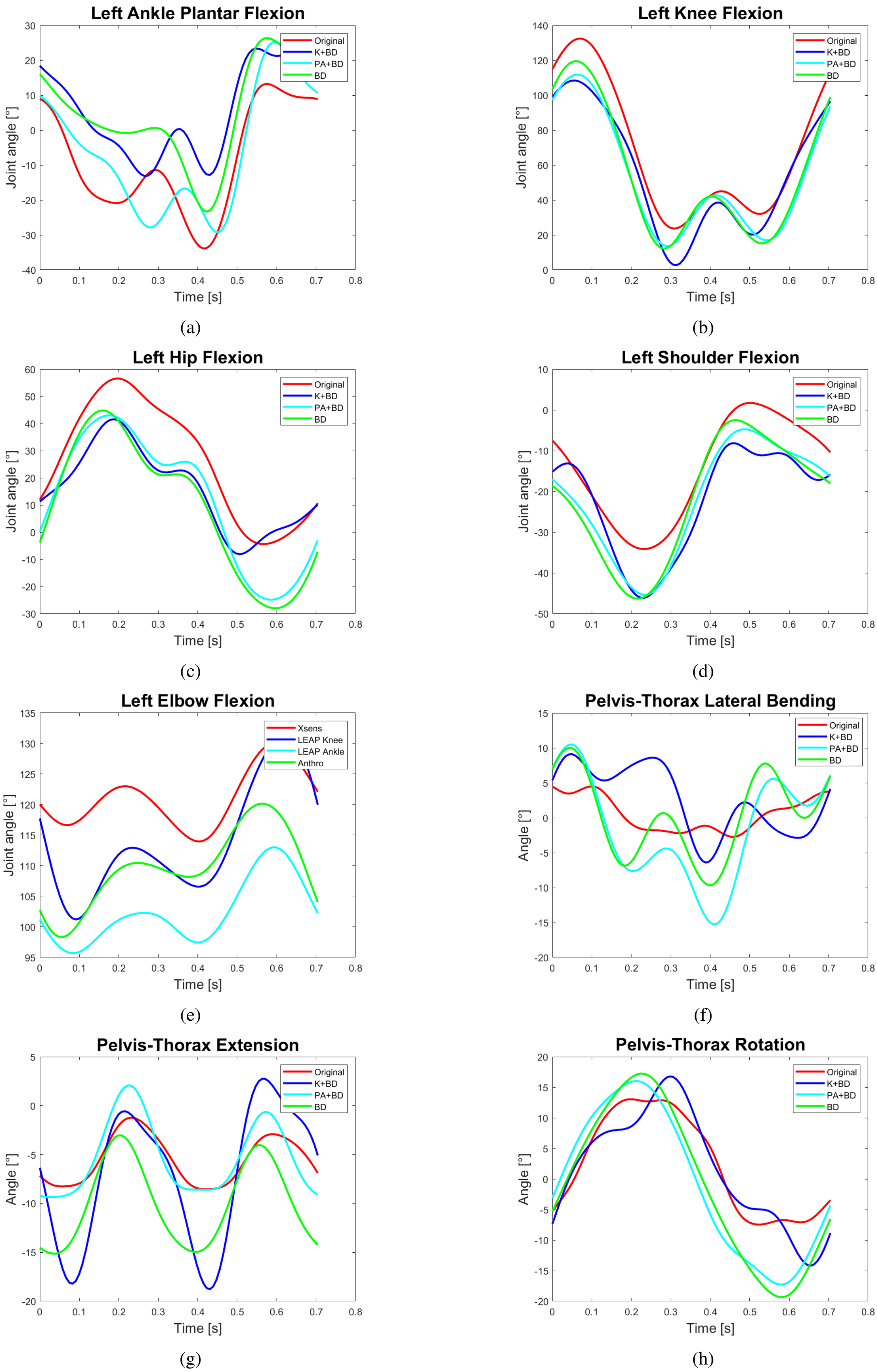

Fig. 6: *Running model predictions for selected variables from the left side and pelvis-thorax using different input options plotted against Xsens. Subject 3, high knee flexion, is used for illustration. Remaining data for subject 3 can be found in Appendix 3.*

Table 7: *Relative prediction error, individually predicted using PA, K, or BD as input for the running model. RPE = Relative prediction error, LF = Low knee flexion, HF = High knee flexion, FF = Forefoot running, PA = Posterior ankle joint sensor, K = Knee joint sensor, BD = Basic data, PT = Pelvis-Thorax, EX = Extension, LB = Lateral bending, ROT= Rotation, F = Flexion, R = Right, L = Left.*

RPE (%)	**LF BD+PA**	**LF BD+K**	**LF BD**	**HF BD+PA**	**HF BD+K**	**HF BD**	**FF BD+PA**	**FF BD+K**	**FF BD**	**All BD+PA**	**All BD+K**	**All BD**
PT EX	79.5	99.4	69.0	35.4	43.5	50.3	54.9	72.0	68.9	56.6	71.6	62.7
PT LB	101.6	129.4	153.4	153.3	133.4	148.8	139.4	160.2	147.6	131.5	141.0	149.9
PT ROT	108.5	113.5	99.8	55.2	46.8	53.4	39.1	69.2	29.3	67.6	76.5	60.8
R Shoulder F	88.3	131.9	123.7	63.3	116.1	82.8	76.6	79.5	74.8	76.1	109.2	93.7
R Elbow F	41.6	30.6	35.2	28.7	25.9	24.6	29.9	29.5	26.6	33.4	28.7	28.8
R Hip F	57.1	52.7	56.3	31.0	51.4	48.3	42.3	43.7	45.0	43.5	49.3	49.9
R Knee F	17.0	17.4	22.7	19.7	24.0	18.1	23.1	19.2	12.5	19.9	20.2	17.8
R Ankle F	53.4	80.4	105.7	60.7	101.6	103.5	103.7	110.2	114.3	72.6	97.4	107.8
L Shoulder F	99.7	159.7	155.0	87.5	101.3	85.1	84.8	99.6	92.4	90.6	119.2	110.8
L Elbow F	30.8	20.9	27.1	22.2	15.9	18.9	16.9	14.6	13.8	23.3	17.1	19.9
L Hip F	60.7	49.8	59.1	35.7	47.5	55.4	44.0	45.1	54.0	46.8	47.5	56.2
L Knee F	15.2	21.0	23.2	20.5	24.9	20.7	24.2	22.3	17.0	19.9	22.7	20.3
L Ankle F	47.9	87.8	103.2	56.2	101.9	94.7	89.0	100.2	90.6	64.4	96.6	96.2
Mean RPE	61.6	76.3	79.5	51.5	64.2	61.9	59.1	66.6	60.5	57.4	69.0	67.3

upper body or arms, it would probably be beneficial since the prediction of these categories have RPEs above average.

3.2 Cross validation and predictions using stretch sensor data

108 kinematic measures were evaluated during cross validation, while only 13 kinematic measures were evaluated from the stretch sensor data. Therefore, RPEs in table 1 cannot be compared directly to RPEs in table 7. However the 13 kinematic measures represented important kinematic parameters for the three categories used in the cross validation. Therefore, it is reasonable to expect the same ranking of the predictions. When comparing the rankings of the predictions they do not match. From the cross validation, right knee + BD provided the best predictions followed by right ankle + BD and then BD. The ranking using stretch sensor input was right ankle + BD followed by BD and then right knee + BD. Most likely, this discrepancy existed because the joint angles measured with the stretch sensors did not match the gold standard. It will be further discussed how the stretch sensors performed in relation to measurement of joint angles.

3.3 Calibration

Figure 3 illustrates the joint angle histories from the calibration process which visually reflects the results observed in table 3. All nine calibration files both AA, PA and K performed great R^2-values ($R^2 > 0.9$), which created a good foundation for translating capacitance measures to joint angles. However, figure 3(a) indicates noticeable differences between measurement methods. This can be a result of interference with the shoe tongue, which could prevent AA from shortening and thereby influence the quadratic function and hence the accuracy of AA. This observation is reflected in table 4, where the RMSE(MAD) of AA (2.67°(8.07°)) was the highest compared to PA (1.17°(3.33°)) and K (1.15°(5.33°)) for subject 3.

Figure 4(a-c) show the knee flexion measured with Xsens and K for the three different running styles. For all running styles it can be observed that peak flexion for K was underestimated compared to Xsens and that the flexion during toe-off was overestimated. These differences could be caused by soft tissue artifacts. The sensor was attached directly on the skin using tape and velcro fasteners. This caused the sensor to pull in the skin when stretched. During quasi-static calibration the sensor stretch was constant, hence the stretch of the skin was constant. When changing to dynamic motion the stretch changed since the knee flexion changed constantly. Both the skin and the stretch sensor have visco-elastic properties which means that when stretching the material it does not return to its original position in the same way as it was stretched [21]. This could explain some of the differences between Xsens and K. Therefore, using a more advanced way of converting capacitance to joint angles could yield better results.

3.4 Sources of interference

Table 5 shows RMSE across running styles for all three sensors. When comparing AA to PA, all RMSE-values for AA were larger than all RMSE-values for PA. When looking at figure 4(d-i) it can also be observed that a larger discrepancy, between the two measurement methods, was present for AA compared to PA. Based on that information AA was not further analysed.

Heel strike for both PA LF and PA HF seem to have been affected by external factors, cf. figure 4(d,e). It seems reasonable that this discrepancy was caused by the heel cap of the shoe, extending the stretch sensor causing an elevation of capacitance for every heel strike. This theory is supported when observing PA FF, cf. figure 4(f). PA FF do not seem to have been influenced by the same elevation when landing. However, PA seemed able to reliably distinguish between LF/HF and FF. To fully investigate the stretch sensor's struggle of measuring heel strike, a barefooted run might provide nuanced information.

Despite obvious differences between Xsens data and stretch sensor data, it cannot be rejected that BD and data from stretch sensor can provide better predictions than using only BD. Both K and PA showed patterns similar to Xsens, cf. figure 4, hence some of the information given to the running model will be correct. Therefore, it was decided to make predictions with the stretch sensor data to test this assumption.

3.5 Predicting using stretch sensor data

The conversion from time series data to Fourier series is seen in figure 5 and table 6. These illustrate the convenience of translating joint angle output into Fourier series. It is fair to state that the conversion to Fourier series using 11 coefficients was successful with R^2-values between 0.971 and 0.999, cf. table 6. This provided a valid foundation in the further assessment of the usability of stretch sensor data in the running model. However, the running model produced unrealistic full body kinematics. In figure 4 it can be observed that the measurement from the stretch sensors were not completely correct. Providing the model with erroneous joint angle histories resulted in unrealistic full body kinematics. It was chosen to reduce the number of Fourier coefficients, given as input in the running model, until realistic full body kinematics were present based on visual feedback from The AnyBody Modeling System. Reducing the number of coefficients given to the model allowed it to predict the remaining coefficients, meaning that the main features of the joint angle history were given as input and that the model predicted the features which the stretch sensor did not measure correctly. No trials needed less then five Fourier coefficients based on stretch sensor conversions. By doing this, this study followed the suggestions of using 11 Fourier coefficients to accurately capture joint angles [13], but varied the amount of coefficients that were based on stretch sensor conversions and coefficients predicted by the running model. Whether this created running model predictions of better or worse quality is uncertain, but it allowed running model predictions using PA + BD as input to predict with lower RPE than BD, cf. table 7.

3.6 Conclusion

In conclusion, the LEAP Technology stretch sensor did not, in this setup, have the ability to correctly measure right knee- and right ankle joint angles but showed similar patterns in joint angles histories, when compared to Xsens MVN Link. However, using a stretch sensor placed posteriorly on the ankle measuring the joint angle provided better predictions from the human running model when combining the data with BD than using only BD based on 13 kinematic measures important for running.

In the current setup, using joint angles measured with the stretch sensors as input in the running model, the predictions are not sufficiently accurate for estimating trial specific biomechanics. It is worth noting, that RPE for the human running model with perfectly measured joint angles was above 50%, cf. table 1, meaning that further development of the human running model is needed to produce more accurate predictions.

3.7 Future studies

To gain further knowledge of which variables are needed, as input in the human running model to obtain precise predictions, a cross validation study combining various inputs would be useful. This knowledge could give rise to new wearables measuring the variables identified as being the best input. The LEAP Technology stretch sensor could also be used to measure other joint angles, e.g. the elbow, if these measures would provide better input. Furthermore, it would be interesting if other more advanced calibration methods or implementation of the stretch sensor in smart textile would provide more precise joint angle measurements during dynamic motion such as running.

4 Acknowledgement

We would like to thank John Rasmussen, Professor, PhD, for his assistance and supervising during our master thesis period.

5 REFERENCES

[1] E. F. Chakravarty, H. B. Hubert, V. B. Lingala, J. F. Fries, "Reduced disability and mortality among aging runners: a 21-year longitudinal study," *Archives of internal medicine*, vol. 168, no. 15, pp. 1638–1646 (2008).

[2] L. Hespanhol Junior, W. Van Mechelen, E. Postuma, E. Verhagen, "Health and economic burden of running-related injuries in runners training for an event: A prospective cohort study," *Scandinavian journal of medicine & science in sports*, vol. 26, no. 9, pp. 1091–1099 (2016).

[3] R. K. Fukuchi, C. A. Fukuchi, M. Duarte, "A public dataset of running biomechanics and the effects of running speed on lower extremity kinematics and kinetics," *PeerJ*, vol. 5, p. e3298 (2017).

[4] L. M. Anderson, D. R. Bonanno, H. F. Hart, C. J. Barton, "What are the benefits and risks associated with changing foot strike pattern during running? A systematic review and meta-analysis of injury, running economy, and biomechanics," *Sports Medicine*, vol. 50, no. 5, pp. 885–917 (2020).

[5] B. Kluitenberg, M. van Middelkoop, R. Diercks, H. van der Worp, "What are the differences in injury proportions between different populations of runners? A systematic review and meta-analysis," *Sports medicine*, vol. 45, no. 8, pp. 1143–1161 (2015).

[6] E. R. Boyer, T. R. Derrick, "Select injury-related variables are affected by stride length and foot strike style during running," *The American journal of sports medicine*, vol. 43, no. 9, pp. 2310–2317 (2015).

[7] M. D. Dunn, D. B. Claxton, G. Fletcher, J. S. Wheat, D. M. Binney, "Effects of running retraining on biomechanical factors associated with lower limb injury," *Human movement science*, vol. 58, pp. 21–31 (2018).

[8] R. A. Gallo, M. Plakke, M. L. Silvis, "Common leg injuries of long-distance runners: anatomical and biomechanical approach," *Sports health*, vol. 4, no. 6, pp. 485–495 (2012).

[9] J. R. Yong, A. Silder, K. L. Montgomery, M. Fredericson, S. L. Delp, "Acute changes in foot strike pattern and cadence affect running parameters associated with tibial stress fractures," *Journal of biomechanics*, vol. 76, pp. 1–7 (2018).

[10] M. Gholami, C. Napier, C. Menon, "Estimating Lower Extremity Running Gait Kinematics with a Single Accelerometer: A Deep Learning Approach," *Sensors*, vol. 20, no. 10, p. 2939 (2020).

[11] V. Hernandez, D. Dadkhah, V. Babakeshizadeh, D. Kulić, "Lower body kinematics estimation from wearable sensors for walking and running: A deep learning approach," *Gait & Posture*, vol. 83, pp. 185–193 (2021).

[12] J. Rasmussen, M. Lund, R. Waagepetersen, "Data-based parametric biomechanical models for cyclic motions," presented at the L. Hanson, D. Hogberg, E. Brolin (Eds.), *DHM 2020 - Proceedings of the 6th International Digital Human Modeling Symposium*, Advances in Transdisciplinary Engineering, pp. 372–379 (2020 Aug.), [Online]. Available: 10.3233/ATDE200045, 6th International Digital Human Modeling Symposium, DHM 2020 ; Conference date: 31-08-2020 Through 02-09-2020.

[13] S. D. Skejø, M. E. Lund, M. Stensvig, N. M. Kaae, J. Rasmussen, "Running in circles: Describing running kinematics using Fourier series," *Journal of Biomechanics*, vol. 115, p. 110187 (2020).

[14] C. Napier, J.-F. Esculier, M. A. Hunt, "Gait retraining: out of the lab and onto the streets with the benefit of wearables," (2017).

[15] G. Aroganam, N. Manivannan, D. Harrison, "Review on wearable technology sensors used in consumer sport applications," *Sensors*, vol. 19, no. 9, p. 1983 (2019).

[16] "Stretch sensor kit,," (2021 May), URL `https://leaptechnology.com/product/stretch-sensors-kit/`.

[17] M. Totaro, T. Poliero, A. Mondini, C. Lucarotti, G. Cairoli, J. Ortiz, L. Beccai, "Soft smart garments for lower limb joint position analysis," *Sensors*, vol. 17, no. 10, p. 2314 (2017).

[18] "Xsens User Manual," (2021 Apr.), URL `https://www.xsens.com/hubfs/Downloads/usermanual/MVN_User_Manual.pdf`.

[19] M. Schepers, M. Giuberti, G. Bellusci, *et al.*, "Xsens mvn: Consistent tracking of human motion using inertial sensing," *Xsens Technol*, pp. 1–8 (2018).

[20] A. Van den Bogert, J. De Koning, "On optimal filtering for inverse dynamics analysis," presented at the *Proceedings of the IXth biennial conference of the Canadian society for biomechanics*, pp. 214–215 (1996).

[21] J. S. Everett, M. S. Sommers, "Skin viscoelasticity: physiologic mechanisms, measurement issues, and application to nursing science," *Biological research for nursing*, vol. 15, no. 3, pp. 338–346 (2013).

THE AUTHORS